

# Theory of Cherenkov radiation in periodic dielectric media: Emission spectrum

Christian Kremers, Dmitry N. Chigrin, and Johann Kroha  
*Physikalisches Institut, Universität Bonn, Nussallee 12, D-53115 Bonn, Germany*

The Cherenkov radiation is substantially modified in the presence of a medium with a nontrivial dispersion relation. We consider Cherenkov emission spectra of a point or line charge, respectively, moving in general, three- (3D) and two-dimensional (2D) photonic crystals. Exact analytical expressions for the spectral distribution of the radiated power are obtained in terms of the Bloch mode expansion. The resulting expression reduces to a simple contour integral (3D case) or a one-dimensional sum (2D case) over a small fraction of the reciprocal space, which is defined by the generalized Cherenkov condition. We apply our method to a specific case of a line source moving with different velocities in a 2D square-lattice photonic crystal. Our method demonstrates a reasonable agreement with numerically rigorous finite-difference time-domain calculations while being less demanding on computational resources.

79.20.2m, 42.70.Qs, 41.60.Bq

## I. INTRODUCTION

Back in 1934 Cherenkov reported the observation of the electromagnetic radiation produced by an electron moving in a dielectric medium at a velocity greater than the phase velocity of light in this medium (author?) [1]. Such a radiation possesses a unique angular and frequency spectrum and is called *Cherenkov radiation* (author?) [2]. A nontrivial dispersion relation of a medium leads to substantial modifications of the Cherenkov radiation. It has been shown that an electron moving in a homogeneous medium with dispersion should emit at any velocity (author?) [3]. Richer spatial distribution of the emitted radiation including intensity oscillations behind the Cherenkov cone is a signature of the radiation in such a medium (author?) [4, 5, 6].

To understand the properties of the Cherenkov radiation one can represent the moving electron with space-time dependence of the corresponding current density  $\mathbf{J}(\mathbf{r}, t) \sim \delta^3(\mathbf{r} - \mathbf{v}t)$  as a superposition of plane waves  $\delta^3(\mathbf{r} - \mathbf{v}t) = \sum_{\mathbf{k}} \exp(i\mathbf{k} \cdot \mathbf{r} - i\mathbf{k} \cdot \mathbf{v}t)$  with different wave vectors  $\mathbf{k}$  and frequency  $\mathbf{k} \cdot \mathbf{v}$ , where  $\mathbf{v}$  is the electron velocity. Only plane waves with frequency and wave vector fitting the medium dispersion  $\omega(\mathbf{k})$  can resonantly excite electromagnetic modes in the medium, which gives the Cherenkov resonance condition (author?) [7]:

$$\omega(\mathbf{k}) = \mathbf{k} \cdot \mathbf{v}. \quad (1)$$

In a homogeneous, non-dispersive medium with refractive index  $n$ , the dispersion relation is simply given by  $\omega(\mathbf{k}) = (c/n)|\mathbf{k}|$  and the Cherenkov condition (1) leads to a well known conical wave front with an aperture  $\cos \phi = c/(n|\mathbf{v}|)$  and a condition on the electron velocity  $|\mathbf{v}| > c/n$  (author?) [2, 7],  $c$  being the vacuum speed of light. In an inhomogeneous medium the interplay between interference and propagation can result in an engineered nontrivial dispersion relation  $\omega(\mathbf{k})$ . For example, periodic dielectric media (photonic crystals) (author?) [8, 9] substantially modify both dispersion and diffraction

of electromagnetic waves possessing many unusual and novel optical phenomena, including modification of emission dynamics (author?) [10, 11, 12], ultra-refraction (author?) [13, 14, 15, 16] and photon focusing (author?) [17, 18, 19] effects. The present work focuses on an analytical understanding of the influence of a periodic medium on the Cherenkov effect.

Several studies on the modification of the radiation produced by a charged particle moving near or inside periodic dielectric media are available. The Cherenkov radiation in cholesteric liquid crystals has been analysed in Ref. [20]. The modification of the Smith-Purcell radiation has been recently studied both theoretically and experimentally near a surface of a two- (2D) and three-dimensional (3D) photonic crystal (author?) [21, 22, 23, 24, 25]. The Cherenkov radiation generated by an electron moving inside an air pore of a 2D photonic crystal perpendicular to the periodicity plane has been used to map its photonic band structure in Refs. (author?) [26, 27]. In all above mentioned reports, the theoretical analysis of the Cherenkov effect has been done in the plane wave basis. Spatial and spectral modifications of the Cherenkov radiation produced by an electron moving in the periodicity plane of a 2D photonic crystal have been studied in Ref. (author?) [28] using the finite-difference time-domain (FDTD) method. To date, there

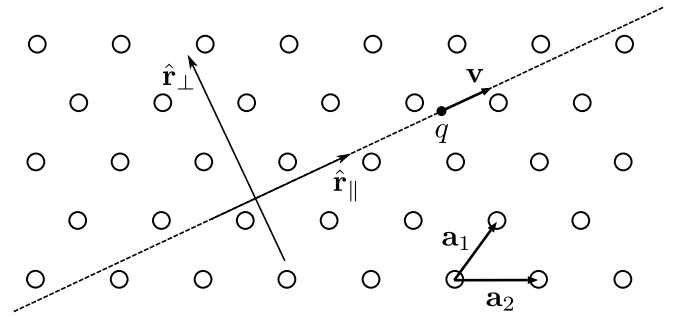


Figure 1: A sketch of a periodic medium and a charge trajectory. Basis vectors  $\mathbf{a}_i$  of the lattice are shown. The coordinate system is chosen with one axis along ( $\hat{\mathbf{r}}_{\parallel}$ ) and the other perpendicular ( $\hat{\mathbf{r}}_{\perp}$ ) to the charge trajectory.

do not exist any reports on the general theory of the Cherenkov effect in an arbitrary 3D periodic dielectric medium [36].

The main purpose of the present work is to develop such a theory and to provide a simple expression for the Cherenkov emission spectrum (energy loss spectrum) for a point or line charge, respectively, moving with velocity  $\mathbf{v}$  in an arbitrary direction inside a general, 3D or 2D photonic crystal. To achieve this goal we derive an analytical expression for the power emitted per unit length of the charge trajectory in terms of the Bloch mode expansion. This expression is further reduced to a simple contour integral (3D case) or a one-dimensional sum (2D case) over a small fraction of the reciprocal space. As a result, to calculate the Cherenkov emission spectrum, Bloch eigenmodes and their corresponding group velocities are required only along an integration path (3D case) or at a discrete set of  $k$ -points (2D case), considerably reducing computational demands. The integration path and the discrete set of points are defined by the generalized Cherenkov condition. Our theory confirms that the Cherenkov radiation does exist in a periodic medium for an arbitrary electron velocity (**author?**) [28]. It also predicts an enhancement of the radiated power near the frequencies corresponding to the vanishing component of the group velocity, which is orthogonal to the electron trajectory.

The paper is organized as follows. In Section II the general solution of Maxwell's equations is summarized for an arbitrary periodic medium. In Section III an analytical expression is derived for the power radiated per unit length by a moving point charge in 3D and a line charge in 2D periodic media. In Section IV we apply our theory to calculate the Cherenkov emission spectra in the

particular case of a 2D photonic crystal. The predictions of the analytical theory are substantiated by numerically rigorous FDTD calculations. Section V concludes the paper.

## II. RADIATED FIELD

We consider a point (line) charge  $q$  uniformly moving with a velocity  $\mathbf{v}$  along some direction in a general, infinite periodic 3D or 2D medium  $\varepsilon(\mathbf{r}) = \varepsilon(\mathbf{r} + \mathbf{R})$  (Fig. 1). Here  $\mathbf{R}$  is a vector of the direct Bravais lattice,  $\mathbf{R} = \sum_i l_i \mathbf{a}_i$ ,  $l_i$  is an integer and  $\mathbf{a}_i$  is a basis vector of the periodic lattice. It is assumed that the medium is linear, nonmagnetic and that no absorption takes place. Then the relevant Maxwell's equations read in SI units:

$$\nabla \times \mathbf{E}(\mathbf{r}, t) = -\mu_0 \frac{\partial}{\partial t} \mathbf{H}(\mathbf{r}, t), \quad (2)$$

$$\nabla \times \mathbf{H}(\mathbf{r}, t) = \varepsilon_0 \varepsilon(\mathbf{r}) \frac{\partial}{\partial t} \mathbf{E}(\mathbf{r}, t) + \mathbf{J}(\mathbf{r}, t), \quad (3)$$

where, the electric (magnetic) field is denoted by  $\mathbf{E}$  ( $\mathbf{H}$ ). An electromagnetic field is produced by a current source  $\mathbf{J}(\mathbf{r}, t)$ , which in the case of the moving point (line) charge is defined as

$$\mathbf{J}(\mathbf{r}, t) = q\mathbf{v}\delta^d(\mathbf{r} - \mathbf{v}t). \quad (4)$$

Here  $d = 2, 3$  is the dimensionality of the periodic lattice. In the frequency domain, a general solution of Maxwell's equations (2-3) for an arbitrary current source  $\mathbf{J}(\mathbf{r}, t)$  and a periodic dielectric function  $\varepsilon(\mathbf{r})$  is given in terms of the Bloch eigenmode expansion (**author?**) [9, 30]

$$\mathbf{E}(\mathbf{r}, \omega) = -i \frac{1}{(2\pi)^d} \frac{\omega}{\varepsilon_0} \sum_n \int_{BZ} d^d k \int d^d r' \left\{ \frac{\mathbf{E}_{\mathbf{k}n}^{(T)}(\mathbf{r}) \otimes \mathbf{E}_{\mathbf{k}n}^{(T)*}(\mathbf{r}')}{\left(\omega - \omega_{\mathbf{k}n}^{(T)} + i\gamma\right) \left(\omega + \omega_{\mathbf{k}n}^{(T)} + i\gamma\right)} + \frac{\mathbf{E}_{\mathbf{k}n}^{(L)}(\mathbf{r}) \otimes \mathbf{E}_{\mathbf{k}n}^{(L)*}(\mathbf{r}')}{\left(\omega + i\gamma\right)^2} \right\} \cdot \mathbf{J}(\mathbf{r}', \omega). \quad (5)$$

Here  $\mathbf{J}(\mathbf{r}, \omega)$  is the Fourier transform of the current density  $\mathbf{J}(\mathbf{r}, t)$ , for the moving point (line) charge (4) given by [37]

$$\mathbf{J}(\mathbf{r}, \omega) = q\hat{\mathbf{r}}_{\parallel} \delta^d(\mathbf{r}_{\perp}) \exp\left(i\omega \frac{r_{\parallel}}{|\mathbf{v}|}\right). \quad (6)$$

The coordinate system is chosen with one axis,  $\hat{\mathbf{r}}_{\parallel}$ , being parallel and other,  $\{\hat{\mathbf{r}}_{\perp}^i\}$ , orthogonal to the electron trajectory (Fig. 1).  $\mathbf{E}_{\mathbf{k}n}^{(T)}(\mathbf{r})$  and  $\mathbf{E}_{\mathbf{k}n}^{(L)}(\mathbf{r})$  are generalized transverse and longitudinal Bloch eigenmodes (**au-**

**thor?**) [9, 30] characterized by the band index  $n$ , the wave vector  $\mathbf{k}$  and the eigenfrequencies  $\omega_{\mathbf{k}n}^{(T)}$  and  $\omega_{\mathbf{k}n}^{(L)}$ , respectively. The Bloch eigenmodes satisfy standard lattice periodic boundary conditions. As it will be shown in the next Section, only transverse Bloch eigenmodes contribute to the Cherenkov radiation field. The asterisk ( $\star$ ) and  $\otimes$  denote the complex conjugate and the outer tensor product in 3D space, respectively. Bloch eigenmodes satisfy the homogeneous wave equation and fulfill the normalization conditions

$$\int d^d r \varepsilon(\mathbf{r}) \mathbf{E}_{\mathbf{k}n}^{(\alpha)\star}(\mathbf{r}) \cdot \mathbf{E}_{\mathbf{k}'n'}^{(\beta)}(\mathbf{r}) = (2\pi)^d \delta_{\alpha\beta} \delta_{nn'} \delta^d(\mathbf{k} - \mathbf{k}') \quad (7)$$

and completeness relations

$$\sum_{n\alpha} \int_{BZ} d^d k \sqrt{\varepsilon(\mathbf{r}) \varepsilon(\mathbf{r}')} \mathbf{E}_{\mathbf{k}n}^{(\alpha)}(\mathbf{r}) \otimes \mathbf{E}_{\mathbf{k}n}^{(\alpha)\star}(\mathbf{r}') = (2\pi)^d \hat{\mathbf{1}} \delta^d(\mathbf{r} - \mathbf{r}'), \quad (8)$$

where  $\alpha, \beta = T$  or  $L$ , and  $\hat{\mathbf{1}}$  is the unit tensor. In Eqs. (5) the  $k$ -space integration is performed over the first Brillouin zone (BZ) of the periodic medium and the summation is carried out over different photonic bands. A positive infinitesimal  $\gamma$  in (5) assures causality (author?) [9].

### III. EMISSION SPECTRUM

The emitted power of the Cherenkov radiation in a general periodic medium is given by the rate at which the moving charge does work on the surrounding electromagnetic field. For an arbitrary current density  $\mathbf{J}(\mathbf{r}, t)$  in a 3D or 2D volume  $V_0$ , the time-dependent emitted power is given by (author?) [31]

$$P(t) = - \int_{V_0} d^d r \mathbf{J}(\mathbf{r}, t) \cdot \mathbf{E}(\mathbf{r}, t). \quad (9)$$

The total energy  $U$  radiated by the current  $\mathbf{J}(\mathbf{r}, t)$  is obtained by integrating (9) over all moments of time

$$U = \int_{-\infty}^{\infty} dt P(t). \quad (10)$$

The time integral in (10) can be further transformed into the integral over frequency (see Appendix A)

$$U = \int_0^{\infty} d\omega P(\omega), \quad (11)$$

with a total power radiated per frequency interval  $[\omega, \omega + d\omega]$  given by

$$P(\omega) = -\frac{1}{\pi} \text{Re} \left[ \int_{V_0} d^d r \mathbf{J}(\mathbf{r}, \omega) \cdot \mathbf{E}^*(\mathbf{r}, \omega) \right]. \quad (12)$$

To obtain the power emitted per unit length of the charge trajectory the integration volume  $V_0$  should be chosen as a cylinder coaxial with the trajectory, while the integral itself should be normalized by the cylinder length  $l$ . In the 2D case, the volume integral is reduced to the surface integral over a rectangle coaxial with the charge trajectory and the result should be normalized to the rectangle length.

We further derive the spectral dependence of the power ( $dP/dl$ ) (12) radiated per unit length by the point (line) charge (4) uniformly moving in a periodic medium. Assuming that the presence of the moving charge does not change the band structure of the periodic medium, the electromagnetic field  $\mathbf{E}(\mathbf{r}, \omega)$  surrounding the moving charge can be expressed in the form of the Bloch eigenmode expansion (5). This expansion is valid for any point  $\mathbf{r}$  in the medium being different from, but as close as required to, the charge trajectory. Substituting the Fourier transform of the current density (6) and the Bloch mode expansion (5) in the equation (12) we obtain

$$\frac{dP}{dl} = -\frac{1}{(2\pi)^d} \frac{\omega}{\pi \varepsilon_0} \sum_n \int_{BZ} d^d k \text{Re} \left[ -i \left\{ \frac{I^{(T)}}{(\omega - \omega_{\mathbf{k}n}^{(T)} + i\gamma)(\omega + \omega_{\mathbf{k}n}^{(T)} + i\gamma)} + \frac{I^{(L)}}{(\omega + i\gamma)^2} \right\} \right] \quad (13)$$

with

$$I^{(\alpha)} = q^2 I_1^{(\alpha)} I_2^{(\alpha)} = q^2 \left\{ \int_{-\infty}^{\infty} dr_{\parallel} \left( \mathbf{e}_{\mathbf{k}n}^{(\alpha)\star}(r_{\parallel}) \cdot \hat{\mathbf{r}}_{\parallel} \right) e^{-i(k_{\parallel} - \frac{\omega}{|\mathbf{v}|})r_{\parallel}} \right\} \left\{ \frac{1}{l} \int_{-l/2}^{l/2} dr_{\parallel} \left( \mathbf{e}_{\mathbf{k}n}^{(\alpha)}(r_{\parallel}) \cdot \hat{\mathbf{r}}_{\parallel} \right) e^{i(k_{\parallel} - \frac{\omega}{|\mathbf{v}|})r_{\parallel}} \right\}, \quad (14)$$

where  $\alpha = T, L$ . We have readily performed the

space integration in the transverse direction  $\hat{\mathbf{r}}_{\perp}$  and used

the Bloch theorem  $\mathbf{E}_{\mathbf{kn}}^{(\alpha)}(\mathbf{r}) = \mathbf{e}_{\mathbf{kn}}^{(\alpha)}(\mathbf{r}) \exp(i\mathbf{k} \cdot \mathbf{r})$ , where  $\mathbf{e}_{\mathbf{kn}}^{(\alpha)}(\mathbf{r})$  is a lattice periodic function. To avoid having to deal with the “bremsstrahlung” radiation we limit ourselves to the electron trajectories which do not cut dielectric interfaces in the periodic medium. Such trajectories are necessarily rationally oriented with respect to the periodic lattice. In this case the function  $(\mathbf{e}_{\mathbf{kn}}^{(\alpha)}(r_{\parallel}) \cdot \hat{\mathbf{r}}_{\parallel})$  in (14) as well as its complex conjugate are both one dimensional periodic functions with a period  $a$  defined by a particular orientation of the electron trajectory. Then, Eq. (14) can be further simplified to (see Appendix B)

$$I^{(\alpha)} = 2\pi q^2 \sum_m \left| c_m^{(\alpha)}(\mathbf{k}; n) \right|^2 \delta \left( k_{\parallel} - \frac{\omega}{|\mathbf{v}|} - \frac{2\pi}{a} m \right). \quad (15)$$

Here  $k_{\parallel}$  is the component of the wave vector parallel to the electron trajectory.  $c_m(\mathbf{k}; n)$  is the  $m$ -th ( $m \in \mathbb{Z}$ ) Fourier coefficient of the periodic function  $(\mathbf{e}_{\mathbf{kn}}^{(\alpha)}(r_{\parallel}) \cdot \hat{\mathbf{r}}_{\parallel})$  defined as

$$c_m^{(\alpha)}(\mathbf{k}; n) = \frac{1}{a} \int_0^a dr_{\parallel} (\mathbf{e}_{\mathbf{kn}}^{(\alpha)}(r_{\parallel}) \cdot \hat{\mathbf{r}}_{\parallel}) e^{-i\frac{2\pi}{a} m r_{\parallel}}. \quad (16)$$

Taking into account the expression (15) and the relation  $\text{Re}[i(\text{Re}[z] + i\text{Im}[z])] = -\text{Im}[z]$ , the power radiated by a moving charge per unit length is given by

$$\frac{dP}{dl} = -\frac{1}{(2\pi)^{d-1}} \frac{\omega q^2}{\pi \varepsilon_0} \sum_{nm} \int_{BZ} d^d k \delta \left( k_{\parallel} - \frac{\omega}{|\mathbf{v}|} - \frac{2\pi}{a} m \right) \left\{ \left| c_m^{(T)}(\mathbf{k}; n) \right|^2 \text{Im} \left[ \frac{1}{(\omega - \omega_{\mathbf{kn}}^{(T)} + i\gamma)(\omega + \omega_{\mathbf{kn}}^{(T)} + i\gamma)} \right] + \left| c_m^{(L)}(\mathbf{k}; n) \right|^2 \text{Im} \left[ \frac{1}{(\omega + i\gamma)^2} \right] \right\}. \quad (17)$$

This expression can be further integrated along the direction  $k_{\parallel}$  in the  $k$ -space yielding

$$\frac{dP}{dl} = -\frac{1}{(2\pi)^{d-1}} \frac{\omega q^2}{\pi \varepsilon_0} \sum_{nm} \int_S d^{d-1} k_{\perp} \left\{ \left| c_m^{(T)}(\mathbf{k}; n) \right|^2 \text{Im} \left[ \frac{1}{(\omega - \omega_{\mathbf{kn}}^{(T)} + i\gamma)(\omega + \omega_{\mathbf{kn}}^{(T)} + i\gamma)} \right] + \left| c_m^{(L)}(\mathbf{k}; n) \right|^2 \text{Im} \left[ \frac{1}{(\omega + i\gamma)^2} \right] \right\}. \quad (18)$$

In the 3D case, a resulting surface integral is taken over a plane  $\mathcal{S}$ . In the 2D case, the integration reduces to an integral over a line  $\mathcal{C}$  (Fig. 2). Both the integration plane and the integration line should be orthogonal to the electron trajectory and are defined by the following relation

$$k_{\parallel} = \frac{\omega}{|\mathbf{v}|} + \frac{2\pi}{a} m. \quad (19)$$

Here the integer  $m$  should be chosen in such a way that

the wave vector  $k_{\parallel}$  stays in the first BZ. Further, taking the limit  $\gamma \rightarrow 0^+$  and using the relation

$$\text{Im} \left[ \lim_{\gamma \rightarrow 0^+} \frac{1}{\omega \pm \omega_{\mathbf{kn}}^{(T)} + i\gamma} \right] = -\pi \delta(\omega \pm \omega_{\mathbf{kn}}^{(T)}), \quad (20)$$

the spectral radiated power (18) can be expressed in the form

$$\frac{dP}{dl} = \frac{1}{(2\pi)^{d-1}} \frac{\omega q^2}{\pi \varepsilon_0} \sum_{nm} \int_S d^{d-1} k_{\perp} \left\{ \frac{\pi}{2\omega_{\mathbf{kn}}^{(T)}} \left| c_m^{(T)}(\mathbf{k}; n) \right|^2 \left( \delta(\omega - \omega_{\mathbf{kn}}^{(T)}) - \delta(\omega + \omega_{\mathbf{kn}}^{(T)}) \right) + \frac{2\pi}{\omega} \left| c_m^{(L)}(\mathbf{k}; n) \right|^2 \delta(\omega) \right\}. \quad (21)$$

The eigenfrequencies of the Bloch modes are positive (**author?**) [8], so the second term in Eq. (21) containing the delta function  $\delta(\omega + \omega_{\mathbf{kn}}^{(T)})$  is zero for all frequencies. The third term in Eq. (21) is due to the work the current

does on the longitudinal part of the electromagnetic field. In the presence of free charges the longitudinal part of the field corresponds to the static electric field and the work done against it results in non-radiative energy transfer with a nonzero contribution only at zero frequency. In what follows we will disregard this non-radiative contribution and will limit ourselves to the radiation into propagating electromagnetic waves only. Then the spectral radiated power is given by

$$\frac{dP}{dl} = \frac{1}{(2\pi)^{d-2}} \frac{\omega q^2}{4\pi\epsilon_0} \sum_{nm} \int_S d^{d-1}k_{\perp} \frac{|c_m^{(T)}(\mathbf{k}; n)|^2 \delta(\omega - \omega_{\mathbf{k}n}^{(T)})}{\omega_{\mathbf{k}n}^{(T)}} \quad (22)$$

The argument of the Dirac delta function in Eq. (22) is a function of the wave vector. One can use this fact to further reduce the dimensionality of the  $(d-1)$   $k$ -space integral. In the 3D case, using the relation

$$\int_{\mathcal{V}} d^d k f(\mathbf{k}) \delta(g(\mathbf{k})) = \int_{\partial\mathcal{V}} d^{d-1}k \frac{f(\mathbf{k})}{|\nabla_{\mathbf{k}} g(\mathbf{k})|}, \quad (23)$$

where  $\partial\mathcal{V}$  is  $(d-1)$  dimensional surface defined by  $g(\mathbf{k}) = 0$ , the integral over the plane  $\mathcal{S}$  is converted into a contour integral

$$\left(\frac{dP}{dl}\right)^{3D} = \frac{q^2}{8\pi^2\epsilon_0} \sum_{nm} \int_{\partial\mathcal{S}} dk \frac{|c_m^{(T)}(\mathbf{k}; n)|^2}{|\nabla_{\mathbf{k}_{\perp}} \omega_{\mathbf{k}n}^{(T)}|}. \quad (24)$$

The contour  $\partial\mathcal{S}$  is defined by the relation (19) and

$$\omega_{\mathbf{k}n}^{(T)} = \omega. \quad (25)$$

It is an intersection of the iso-frequency surface with plane  $\mathcal{S}$  (Fig. 2-top). In the 2D case, the relation

$$\delta(f(k)) = \sum_i \frac{\delta(k - k_i)}{|f'(k_i)|} \quad (26)$$

can be used, where summation is taken over all solutions of the equation  $f(k) = 0$ . Substituting (26) into (22) we obtain

$$\left(\frac{dP}{dl}\right)^{2D} = \frac{\omega q^2}{4\pi\epsilon_0} \sum_{nmi} \int_{\mathcal{C}} dk_{\perp} \frac{|c_m^{(T)}(\mathbf{k}; n)|^2 \delta(k_{\perp} - k_{\perp,i})}{\omega_{\mathbf{k}n}^{(T)} \left( \left| \partial\omega_{\mathbf{k}n}^{(T)} / \partial k_{\perp} \right| \right)_{k_{\perp,i}}}, \quad (27)$$

where  $\{k_{\perp,i}\}$  are simultaneous solutions of the equations (19) and (25) given by the intersections of the iso-frequency contour with the line  $\mathcal{C}$  (Fig. 2-bottom). Performing  $k$ -space integration, we finally obtain

$$\left(\frac{dP}{dl}\right)^{2D} = \frac{q^2}{4\pi\epsilon_0} \sum_{nmi} \left( \frac{|c_m^{(T)}(\mathbf{k}; n)|^2}{\left| \partial\omega_{\mathbf{k}n}^{(T)} / \partial k_{\perp} \right|} \right)_{k_{\perp,i}}, \quad (28)$$

where the function in brackets is calculated for the wave vectors corresponding to the set  $\{k_{\perp,i}\}$ .

Formulas (24) and (28) constitute the main result of the present work. They give the power radiated by the moving point charge (3D) or line charge (2D)  $q$  in the spectral interval  $[\omega, \omega + d\omega]$  per unit length of the trajectory for a 3D and 2D periodic medium, respectively. The radiated power is proportional to the Fourier coefficients  $c_m^{(T)}(\mathbf{k}; n)$ , which effectively describe the local coupling strength between the current density produced by a moving charge and the electromagnetic field at the electron location. The gradient and derivative of the dispersion relation  $\mathbf{v}_{\perp}^g = \nabla_{\mathbf{k}_{\perp}} \omega_{\mathbf{k}n}^{(T)}$  and  $v_{\perp}^g = \partial\omega_{\mathbf{k}n}^{(T)} / \partial k_{\perp}$  yield the component of the group velocity,  $\mathbf{v}^g$ , of the Bloch eigenmode  $(\mathbf{k}; n)$ , which is orthogonal to the electron trajectory. The Cherenkov radiated power is proportional to the inverse of this component of the group velocity. That means that the radiated power can be *strongly enhanced* not only if the group velocity itself is small for some frequency, but also if the component of the group velocity orthogonal to the electron trajectory becomes small. At the same time *suppression* of the Cherenkov radiation is possible if for some frequency the current density produced by a moving charge is not coupled to the corresponding Bloch mode and the Fourier coefficients  $c_m^{(T)}(\mathbf{k}; n)$  is small.

Only eigenmodes with the wave vectors on the contour  $\partial\mathcal{S}$  (24) and from the set  $\{k_{\perp,i}\}$  (28) contribute to the radiated power at a given frequency. It is important to realize that Eqs. (19) and (25) defining the contour  $\partial\mathcal{S}$  and the set  $\{k_{\perp,i}\}$  are equivalent to the Cherenkov resonance condition (1). In fact, substituting (25) in (19) and taking into account that the scalar product in (1) results in  $\mathbf{v} \cdot \mathbf{k} = |\mathbf{v}| k_{\parallel}$  one obtains the *generalized Cherenkov condition* for a periodic medium

$$\omega_{\mathbf{k}n}^{(T)} = |\mathbf{v}| k_{\parallel} - |\mathbf{v}| \frac{2\pi}{a} m. \quad (29)$$

In the 4D (3D)  $(\omega-k)$ -space the right-hand side of the relation (29) defines a hyperplane (plane) whose intersection with the band structure,  $\omega_{\mathbf{k}n}^{(T)}$ , determines Bloch modes contributing to the Cherenkov radiation (Fig. 3-top). Nonzero integers  $m$  ensure that such an intersection and consequently the Cherenkov radiation exist in a periodic medium for an *arbitrarily small* charge velocity. In a homogeneous medium  $m = 0$  and the Cherenkov condition reduces to a standard form  $\omega_{\mathbf{k}} = |\mathbf{v}| k_{\parallel}$ .

As a simple check of our theory we show in the following that the final formulas (24,28) reproduce the limit of a homogeneous medium with the dielectric constant  $\varepsilon$ . For a given frequency  $\omega$ , the wave vector  $|\mathbf{k}|$  and the group velocity  $|\mathbf{v}_\perp^g|$  are given by  $|\mathbf{k}| = (\omega\sqrt{\varepsilon})/c$  and  $|\mathbf{v}_\perp^g| = (c|\mathbf{k}_\perp|)/(\sqrt{\varepsilon}|\mathbf{k}|)$  respectively, with  $\mathbf{k}_\perp = \mathbf{k} - k_\parallel \hat{\mathbf{v}}$  being the component of the wave vector perpendicular to the electron trajectory. The appropriately normalized eigen-

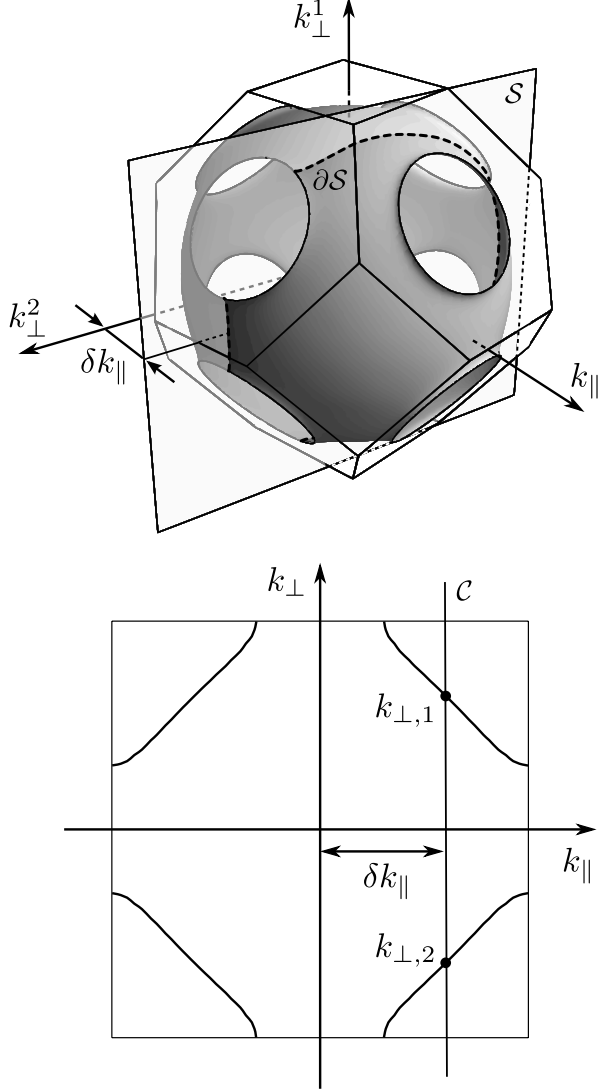


Figure 2: (Top) Diagram to define the integration plane  $S$  and the integration contour  $\partial S$  (dashed line) in Eq. (18,24). Iso-frequency surface enclosed in the first BZ of the FCC lattice is shown for a normalized frequency  $\omega_{\mathbf{k}n} = \omega$  inside the first bandgap of a 3D inverted opal (author?) [32]. (Bottom) Diagram to define the integration line  $C$  and the set of points  $\{k_{\perp,i}\}$  (two thick dots) in Eqs. (18,28). Iso-frequency contour enclosed in the first BZ of a square lattice PhC is shown for a normalized frequency  $\omega_{\mathbf{k}n} = \omega$  inside the first bandgap. The plane  $S$  and the line  $C$  are defined by the relation  $k_\parallel = \delta k_\parallel = \frac{\omega}{|\mathbf{v}|} + \frac{2\pi}{a}m$ . The choice of the coordinate system with one axis,  $k_\parallel$ , parallel to the electron trajectory is shown.

modes are plane waves  $\mathbf{E} = (1/\sqrt{\varepsilon}) \hat{\mathbf{e}} \exp(i\mathbf{k} \cdot \mathbf{r})$ , where  $\hat{\mathbf{e}}$  is a polarization unit vector orthogonal to the wave vector  $\mathbf{k}$ . Further, according to the Eq. (19) the wave vector component  $k_\parallel$  is equal to  $k_\parallel = \omega/|\mathbf{v}|$  with  $m = 0$  and the coefficient  $c_0$  is given by  $c_0 = |\mathbf{k}_\perp|/(\sqrt{\varepsilon}|\mathbf{k}|)$ . Then in the 3D case, taking into account that an integration contour  $\partial S$  is a circle of radius  $|\mathbf{k}_\perp|$  and performing integration in polar coordinates with  $d\mathbf{k} = |\mathbf{k}_\perp| d\phi$ , the radiated power

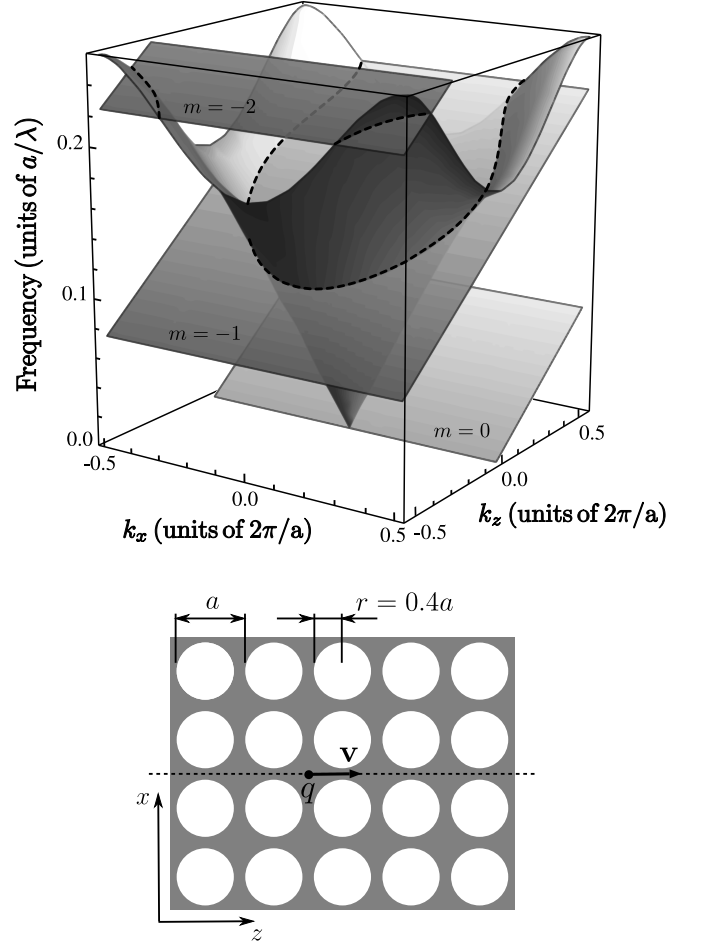


Figure 3: Diagram to illustrate the generalized Cherenkov condition (29). A 3D representation of the photonic band structure (top) of the 2D PhC (bottom) is shown for TE polarization. An infinite 2D square lattice of air holes in a dielectric medium is considered. The radius of the holes is  $r = 0.4a$ , the dielectric constant of the background medium is  $\varepsilon = 12.0$ . Only the first band in the first BZ is presented. The right-hand side of Eq. (29) defines the set of planes for different  $m$ . The intersection (dashed line) of these planes with the band structure determines the Bloch modes contributing to the Cherenkov radiation. Here it is supposed that a line charge moves along the  $z$ -axis in the crystal with velocity  $|\mathbf{v}| = 0.15c$ .

(24) is given by

$$\left(\frac{dP}{dl}\right)_h^{3D} = \frac{1}{4\pi\epsilon_0} \frac{q^2}{c\sqrt{\epsilon}} |\mathbf{k}| \left(1 - \left(\frac{|\mathbf{k}_{||}|}{|\mathbf{k}|}\right)^2\right), \quad (30)$$

which finally yields the usual results of the Frank-Tamm theory (author?) [7]

$$\left(\frac{dP}{dl}\right)_h^{3D} = \frac{q^2\omega}{4\pi\epsilon_0 c^2} \left(1 - \frac{c^2}{\epsilon |\mathbf{v}|^2}\right). \quad (31)$$

In the 2D case Eq. (28) yields

$$\left(\frac{dP}{dl}\right)_h^{2D} = \frac{1}{2\pi\epsilon_0} \frac{q^2}{c\sqrt{\epsilon}} \sqrt{1 - \frac{c^2}{\epsilon |\mathbf{v}|^2}}. \quad (32)$$

#### IV. NUMERICAL RESULTS

In this section the analytical results developed in the previous section are applied to the numerical study of the Cherenkov radiation in a 2D photonic crystal. An infinite 2D square lattice of air holes in a dielectric medium is considered. The radius of the holes is  $r = 0.4a$ , while the dielectric constant of the background medium is  $\epsilon = 12.0$ . A line charge oriented perpendicular to the periodicity plane of the crystal moves along the  $z$ -axis with a velocity  $v$ , staying always in the space between air holes (Fig. 3 bottom). The corresponding current density, Eqs. (4) and (6), generates an electric field (5) polarized in the periodicity plane (transverse electric or TE polarization) (author?) [8, 9], i.e., the Bloch eigenmode expansion should include the TE polarized Bloch modes only. The first TE band for the considered PhC is presented in the figure 3-top. The band structure was calculated using the plane wave expansion method (author?) [33].

To find the power radiated by a charge moving with a given velocity  $v$ , all Bloch modes contributing to the radiation should be determined. These modes are specified by the solutions of the relation (29). In what follows we restrict our analysis to the frequency range of the first band of the considered PhC structure. In figure 3-top, solutions of the Cherenkov relations (29) are graphically illustrated for  $m = 0, -1, -2$  (dashed lines) and charge velocity  $v = 0.15c$ . The frequencies satisfying relations (29) determine the spectral range of nonzero contribution to the Cherenkov radiated power, the *Cherenkov band*. The evolution of the Cherenkov band is presented in figure 4 as a function of the charge velocity.

For charge velocity  $v = 0.15c$ , the Cherenkov spectrum is given by the intersections of the band structure with the planes  $m = -1$  and  $m = -2$ . The plane corresponding to  $m = 0$  does not intersect the band structure of the crystal (Figs. 3, 4). For smaller charge velocities, more and more planes intersect the photonic band structure, and the Cherenkov spectrum is built from a number of

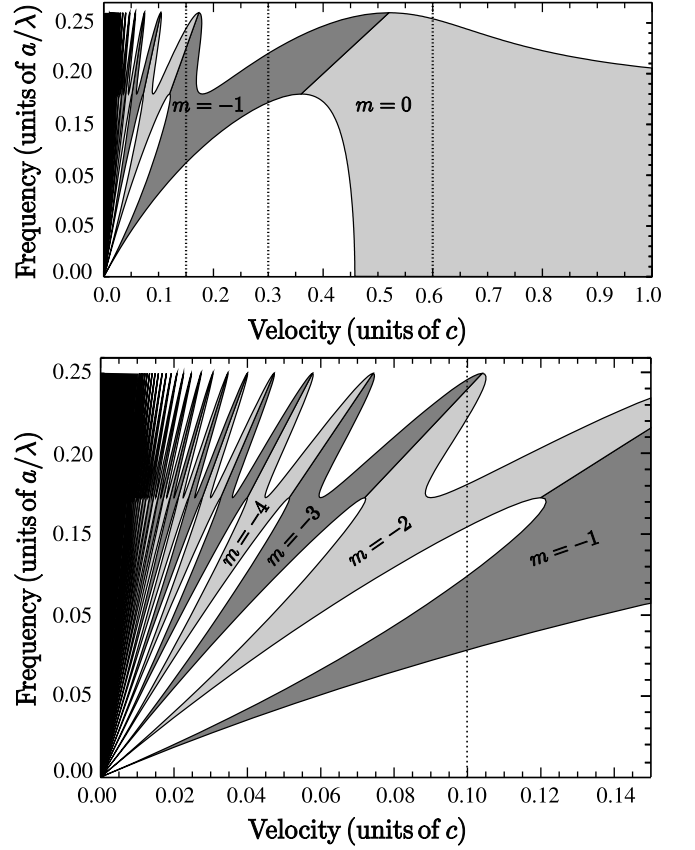


Figure 4: Cherenkov radiation band. Sub-bands defined by the intersections of the band structure with the planes corresponding to the different  $m$ 's are shaded in light and dark gray. Vertical lines mark the charge velocities used in the further calculations,  $v = 0.15c$ ,  $v = 0.3c$  and  $v = 0.6c$  in the top panel and  $v = 0.1c$  in the bottom panels, respectively.

discrete sub-bands. For sufficiently small charge velocities the spectral range of the first photonic band becomes densely filled with the discrete sub-bands (Fig. 4).

In the long wavelength limit the periodic medium is effectively homogeneous. For the PhC considered in Fig. 4 the effective refractive index is equal to  $n_{\text{eff}} = \sqrt{\epsilon_{\text{eff}}} \approx 2.186$ . Consequently, for  $m = 0$  the relation (29) imposes a condition on the minimal charge velocity to produce Cherenkov radiation at small frequencies, namely  $v \geq v_{\text{min}} = c/n_{\text{eff}} \approx 0.457c$ . For charge velocities larger than the threshold value the Cherenkov band covers the spectral range from zero to the maximum frequency, which is defined by the intersection of the band structure with the plane  $m = 0$  at the first BZ boundary (Fig. 4).

To compute the radiated power from Eq. (28), one should calculate the Bloch modes along a charge trajectory, their Fourier transforms and corresponding group velocities for wave vectors belonging to the intersections defined by Eq. (29). The calculation of the Cherenkov spectrum is illustrated in figure 5 for a line charge ( $q = 1.6 \times 10^{-19} C$ ) moving with the velocity  $v = 0.1c$ . To cal-

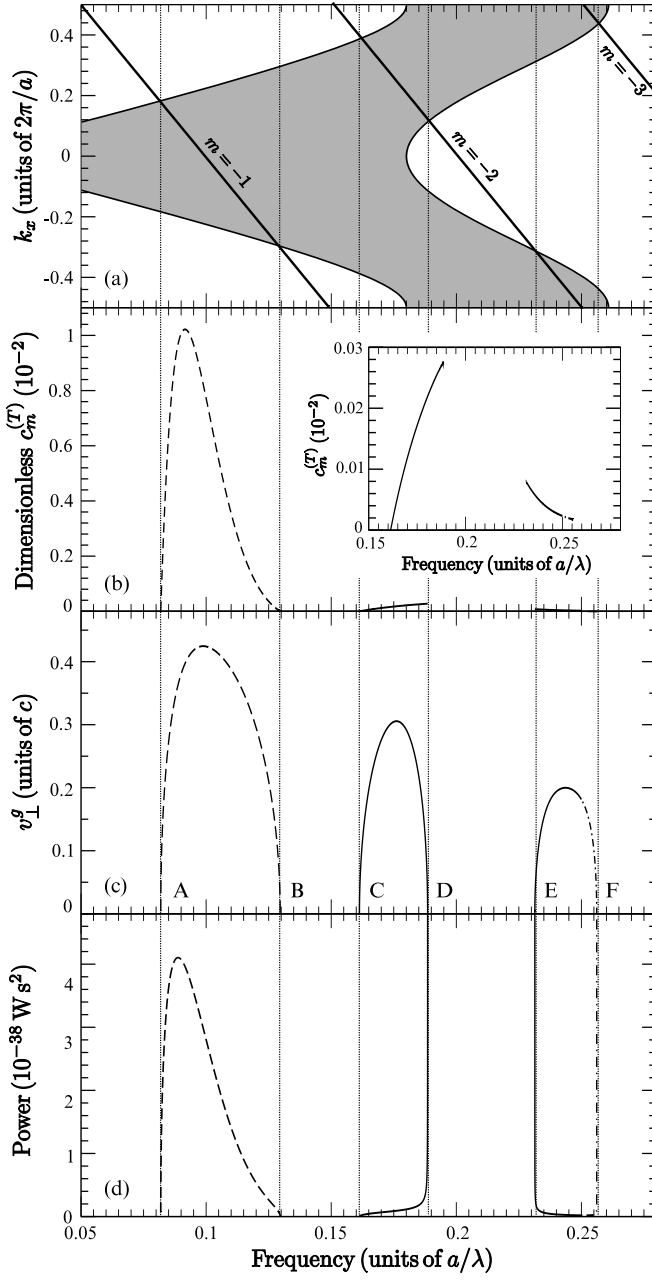


Figure 5: Cherenkov emission spectrum for the charge velocity  $v = 0.1c$ . Projections of the first band of the considered photonic crystal and the planes  $m = -1$ ,  $m = -2$  and  $m = -3$  defining the Cherenkov band on the  $k_x$ - $\omega$  plane are shown (a). The Fourier coefficients,  $c_m^{(T)}(\mathbf{k}; n)$ , the orthogonal component of the group velocity,  $v_{\perp}^g$ , and the Cherenkov power spectrum are shown in panels (b), (c) and (d), respectively. Vertical lines mark the edges of the Cherenkov sub-bands. Contribution from the sub-bands corresponding to  $m = -1$ ,  $m = -2$  and  $m = -3$  are shown as dashed, solid and dashed-dotted lines, respectively.

culate Bloch modes and group velocities, the plane wave expansion method (**author?**) [33] and the Hellmann-Feynman theorem were used, respectively. For the velocity  $v = 0.1c$  the Cherenkov spectrum consists of three sub-bands defined by the planes  $m = -1$ ,  $m = -2$  and  $m = -3$  (Figs. 4, 5), respectively. The Fourier coefficients,  $c_m^{(T)}(\mathbf{k}; n)$ , (Fig. 5-b) and the orthogonal component of the group velocity,  $v_{\perp}^g$ , (Fig. 5-c) are nonzero only within the sub-bands. Both Fourier coefficients and the orthogonal component of the group velocity approach zero at sub-band edges A, B and C. At the edges D, E, and F only the orthogonal component of the group velocity is zero, while the Fourier coefficients have finite nonzero value. Calculation of the Cherenkov radiated power at the band edges A, B and C leads to the indeterminate limits of the form  $0/0$ , which can be evaluated using l'Hopital's rule and is equal to zero. At the band edges D, E and F the Cherenkov power diverges in an integrable way.

In figure 6 the Cherenkov radiated power spectra are shown for charge velocities  $v = 0.15c$ ,  $v = 0.3c$  and  $v = 0.6c$ . For charge velocities smaller than the threshold value  $v_{\min} \approx 0.457c$  the Cherenkov radiation is nonzero only within single or multiple spectral bands. For velocities above the threshold, the radiated power is nonzero almost everywhere within the first band, approaching asymptotically the value of the Cherenkov radiated power in a homogeneous medium with  $n = n_{\text{eff}}$  for small frequencies. The radiated power calculated using Eq. (32) for  $v = 0.6c$  and  $n_{\text{eff}} = 2.186$  is shown in figure 6 (bottom panel) as dotted line. The Cherenkov radiated power is enhanced near those frequencies where the group velocity component orthogonal to the charge trajectory vanishes, while the Fourier coefficients remain finite (Fig. 6).

To substantiate our analytical results the direct numerical integration of the Maxwell's equations has been performed using rigorous finite-difference time-domain (FDTD) method (**author?**) [34]. The simulated structure was a  $10a \times Na$  lattice of air holes in a homogeneous medium with  $\epsilon = 12.0$ . The longitudinal size of the periodic structure was set to  $N = 188$ ,  $N = 376$  and  $N = 752$  lattice constants for an charge velocity  $v = 0.15c$ ,  $v = 0.3c$  and  $v = 0.6c$ , respectively. The lattice was surrounded by a  $2a$  wide layer of homogeneous material. The simulation domain was discretized into squares with a side  $\Delta = a/18$  and was surrounded by a 35-cell-wide perfectly matched layer (PML) (**author?**) [35]. The time step of integration was set to 98% of the Courant value. The moving line source (4) was modeled as a current density source (**author?**) [34] with the Dirac delta function represented via an appropriately normalized Kronecker delta  $\delta_{ij}/\Delta^2$ . The charge trajectory was oriented in the longitudinal direction of the system, placed in the geometrical center of the crystal, exactly between the 5th and the 6th row of holes.

For the numerical computation of the radiated power the electric and magnetic fields were stored at a detector surface enclosing the crystal, and their Fourier trans-



forms with respect to time were found by discrete Fourier transformation. The longitudinal dimension of the structure was different for different charge velocities in order to keep the integration time at the detector and consequently the spectral resolution constant. The detector surface was situated in the close vicinity of the crystal boundary. The total radiated power per unit length was then calculated as

$$\frac{dP}{dl} = \frac{1}{d} \frac{2}{\pi} \int_0^D dz \mathbf{S}(z, \omega) \cdot \hat{\mathbf{n}} \quad (33)$$

where  $\mathbf{S}(z, \omega) = \frac{1}{2} \text{Re} [\mathbf{E}(z, \omega) \times \mathbf{H}^*(z, \omega)]$  is the Poynting vector at radiation frequency  $\omega$ ,  $D$  is the length of the detector surface along the trajectory and  $\hat{\mathbf{n}}$  is a unit vector orthogonal to the detector interface.

An overall very good agreement between the results of the analytical (Fig. 6, solid lines) and numerical calculations (Fig. 6, dashed lines) is obtained. Both the spectral range of a nonzero radiated power and its absolute value are well represented using the FDTD method. The main difference can be traced back to Fabry-Perot-like oscillations of the radiated power due to the finite-size effects in the FDTD calculations. In the finite structure, the Cherenkov radiated power stays considerably enhanced near the band edges having large but finite value. The total power oscillates around the analytical value becoming partially suppressed or enhanced for different frequencies. To confirm that these oscillations indeed result from the finite transverse dimension of the considered photonic crystal, we have performed simulations for the crystal with a double thickness ( $20a \times 188a$ ) for the charge velocity  $v = 0.15c$ . Resulting radiated power spectrum is shown in the corresponding panel in figure 6 as a dashed-dotted curve. One can see twice as many oscillations as in the case of the thinner structure, which is a typical signature of the Fabry-Perot like phenomena. The further enhancement of the radiated power in comparison to the infinite structure can be associated with the longer interaction time of the charge at resonance frequencies with the effectively slow Fabry-Perot modes of a photonic crystal slab.

## V. CONCLUSIONS

In this paper, analytical expression for the Cherenkov power emitted per unit length of the charge trajectory in the case of a general 3D and 2D periodic dielectric medium has been derived. The obtained formula for the Cherenkov power involves the calculations of Bloch modes and corresponding group velocities at a limited number of points of the reciprocal space only, making the application of the proposed method computationally not demanding. All calculations have been performed on a desktop PC and our method requires 5 to 10 times less CPU time than FDTD method. The analysis of the Cherenkov emission spectrum in the periodic medium

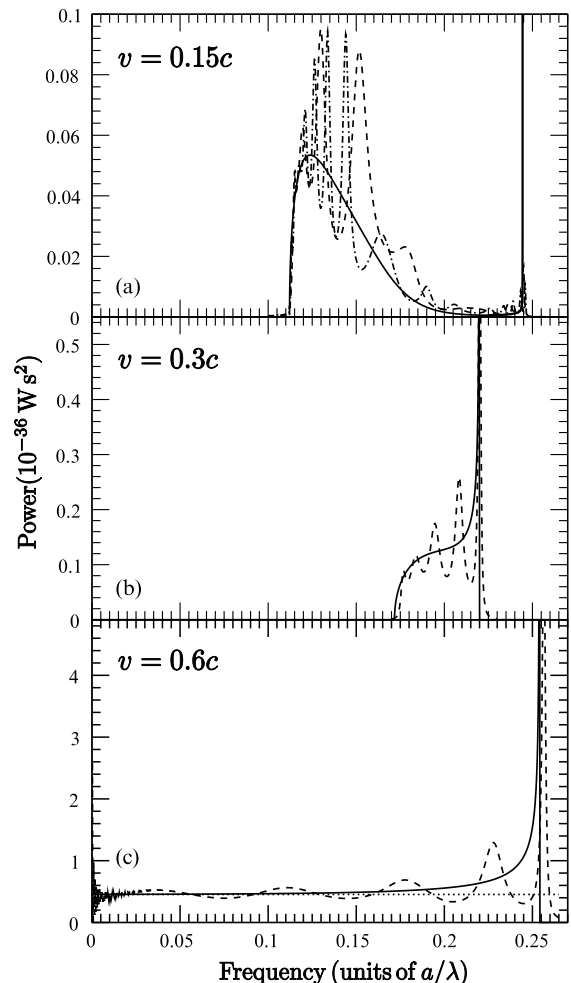


Figure 6: Cherenkov emission spectra for different charge velocities in a 2D photonic crystal. Solid lines correspond to the analytical results (28). Dotted line in the bottom panel ( $v = 0.6c$ ) corresponds to the Cherenkov radiated power in the homogeneous medium with  $n_{\text{eff}} = 2.186$ , Eq. (32). Radiated power spectra obtained using FDTD method are shown as dashed lines. For charge velocity  $v = 0.15c$  radiated power spectra are shown for both  $10a \times 188a$  (dashed line) and  $20a \times 188a$  (dashed-dotted line) structures.

reveals that the Cherenkov effect indeed exists for every electron velocity. Similar to the case of the modification of the dipole emission in a photonic crystal, the Cherenkov radiation can be suppressed if the coupling of the current density produced by a moving electron with a Bloch mode is poor. At the same time, an enhancement of the Cherenkov radiation is possible also if only the component of the group velocity orthogonal to the electron trajectory is small. We have illustrated the developed analytical method and its conclusions using a numerically rigorous finite-difference time-domain method in a special case of a 2D photonic crystal and demonstrated a reasonable agreement between numerical and analytical results.

### Acknowledgments

We are grateful to Sergei Zhukovsky for fruitful discussions and careful reading of the manuscript. Financial support from the Deutsche Forschungsgemeinschaft (DFG FOR 557) is gratefully acknowledged.

### Appendix A

Using the Fourier representation of the time depended real function  $\mathbf{F}(\mathbf{r}, t)$ ,

$$\begin{aligned}\mathbf{F}(\mathbf{r}, t) &= \text{Re} \left[ \frac{1}{2\pi} \int_{-\infty}^{\infty} d\omega \mathbf{F}(\mathbf{r}, \omega) e^{-i\omega t} \right] \\ &= \frac{1}{4\pi} \int_{-\infty}^{\infty} d\omega (\mathbf{F}(\mathbf{r}, \omega) e^{-i\omega t} + \mathbf{F}^*(\mathbf{r}, \omega) e^{i\omega t}),\end{aligned}\quad (34)$$

for the electric field  $\mathbf{E}(\mathbf{r}, t)$  and the current density  $\mathbf{J}(\mathbf{r}, t)$  in Eq. (9), the total radiated energy (10) can be written in the form

$$\begin{aligned}U &= -\frac{2}{(4\pi)^2} \text{Re} \left[ \int_{V_0} d^d r \int_{-\infty}^{\infty} dt \int_{-\infty}^{\infty} d\omega \int_{-\infty}^{\infty} d\Omega \times \right. \\ &\quad \left\{ \mathbf{J}(\mathbf{r}, \omega) \cdot \mathbf{E}(\mathbf{r}, \Omega) e^{-i(\omega+\Omega)t} + \right. \\ &\quad \left. \mathbf{J}(\mathbf{r}, \omega) \cdot \mathbf{E}^*(\mathbf{r}, \Omega) e^{-i(\omega-\Omega)t} \right\} \Big].\end{aligned}\quad (35)$$

Changing the integration order and using the integral relation for the Dirac delta function

$$\delta(x) = \frac{1}{2\pi} \int_{-\infty}^{\infty} dy e^{-ixy} \quad (36)$$

we obtain for total radiated energy

$$\begin{aligned}U &= -\frac{1}{4\pi} \text{Re} \left[ \int_{V_0} d^d r \int_{-\infty}^{\infty} d\omega \int_{-\infty}^{\infty} d\Omega \times \right. \\ &\quad \left\{ \mathbf{J}(\mathbf{r}, \omega) \cdot \mathbf{E}(\mathbf{r}, \Omega) \delta(\omega + \Omega) + \right. \\ &\quad \left. \mathbf{J}(\mathbf{r}, \omega) \cdot \mathbf{E}^*(\mathbf{r}, \Omega) \delta(\omega - \Omega) \right\} \Big].\end{aligned}\quad (37)$$

Further, integrating over  $\Omega$  and using the symmetry of the Fourier transform of the electric field,  $\mathbf{E}(\mathbf{r}, -\omega) = \mathbf{E}^*(\mathbf{r}, \omega)$ , the total radiated energy can be written as an integral over frequency (11)

$$U = -\frac{2}{\pi} \int_0^{\infty} d\omega \frac{1}{2} \text{Re} \left[ \int_{V_0} d^d r \mathbf{J}(\mathbf{r}, \omega) \cdot \mathbf{E}^*(\mathbf{r}, \omega) \right]. \quad (38)$$

The integrand in Eq. (38) coincides with the time-averaged radiated power of the monochromatic source  $\mathbf{J}(\mathbf{r}, \omega)$  (author?) [31].

### Appendix B

Expanding a periodic function  $(\mathbf{e}_{\mathbf{k}n}^{(\alpha)}(r_{\parallel}) \cdot \hat{\mathbf{r}}_{\parallel})$  in the Fourier series

$$(\mathbf{e}_{\mathbf{k}n}^{(\alpha)}(r_{\parallel}) \cdot \hat{\mathbf{r}}_{\parallel}) = \sum_{m=-\infty}^{\infty} c_m^{(\alpha)}(\mathbf{k}; n) e^{i\frac{2\pi}{a} m r_{\parallel}} \quad (39)$$

with coefficients  $c_m^{(\alpha)}(\mathbf{k}; n)$  defined in Eq. (16), integrals  $I_1^{(\alpha)}$  and  $I_2^{(\alpha)}$  in (14) can be transformed to

$$I_1^{(\alpha)} = \sum_{m=-\infty}^{\infty} c_m^{(\alpha)*}(\mathbf{k}; n) \int_{-\infty}^{\infty} dr_{\parallel} e^{-i(k_{\parallel} - \frac{\omega}{|\mathbf{v}|} - \frac{2\pi}{a} m) r_{\parallel}} \quad (40)$$

and

$$I_2^{(\alpha)} = \sum_{p=-\infty}^{\infty} c_p^{(\alpha)}(\mathbf{k}; n) \frac{1}{l} \int_{-l/2}^{l/2} dr_{\parallel} e^{i(k_{\parallel} - \frac{\omega}{|\mathbf{v}|} - \frac{2\pi}{a} p) r_{\parallel}}, \quad (41)$$

respectively. In Eq. (40), integration over  $r_{\parallel}$  immediately yields

$$I_1^{(\alpha)} = 2\pi \sum_{m=-\infty}^{\infty} c_m^{(\alpha)*}(\mathbf{k}; n) \delta\left(k_{\parallel} - \frac{\omega}{|\mathbf{v}|} - \frac{2\pi}{a} m\right). \quad (42)$$

Integral in (41) is equal to  $l$ , if  $k_{\parallel} - \frac{\omega}{|\mathbf{v}|} - \frac{2\pi}{a} p = 0$ . Otherwise it results in

$$\frac{\sin\left(\left(k_{\parallel} - \frac{\omega}{|\mathbf{v}|} - \frac{2\pi}{a} p\right) (l/2)\right)}{\left(k_{\parallel} - \frac{\omega}{|\mathbf{v}|} - \frac{2\pi}{a} p\right)}. \quad (43)$$

Then, in the limit  $l \rightarrow \infty$ ,  $I_2^{(\alpha)}$  vanishes for  $k_{\parallel} - \frac{\omega}{|\mathbf{v}|} - \frac{2\pi}{a} p \neq 0$ , while is equal to  $2\pi \sum_{p=-\infty}^{\infty} c_p^{(\alpha)}(\mathbf{k}; n)$  for  $k_{\parallel} - \frac{\omega}{|\mathbf{v}|} - \frac{2\pi}{a} p = 0$ . Finally, using the function

$$\tilde{\delta}(x) = \begin{cases} 1, & x = 0 \\ 0, & x \neq 0 \end{cases}, \quad (44)$$

relation (14) can be written in the form

$$\begin{aligned}I^{(\alpha)} &= 2\pi q^2 \sum_{m=-\infty}^{\infty} \sum_{p=-\infty}^{\infty} c_m^{(\alpha)*}(\mathbf{k}; n) c_p^{(\alpha)}(\mathbf{k}; n) \times \\ &\quad \delta\left(k_{\parallel} - \frac{\omega}{|\mathbf{v}|} - \frac{2\pi}{a} m\right) \tilde{\delta}\left(k_{\parallel} - \frac{\omega}{|\mathbf{v}|} - \frac{2\pi}{a} p\right),\end{aligned}\quad (45)$$

which is non-zero only for  $m = p$  yielding relation (15).

- 
- [1] P. A. Cherenkov, Dokl. Acad. Nauk SSSR **2**, 457 (1934).
- [2] J. V. Jelley, *Cherenkov Radiation and its Applications* (Pergamon, New York, 1958).
- [3] E. Fermi, Phys. Rev. **57**, 485 (1940).
- [4] G. N. Afanasiev, V. G. Kartavenko, and E. N. Magar, Physica **B269**, 95 (1999).
- [5] I. Carusotto, M. Artoni, G. C. La Rocca, and F. Bassani, Phys. Rev. Lett. **87**, 064801 (2001).
- [6] M. Artoni, I. Carusotto, G. C. La Rocca, and F. Bassani, Phys. Rev. E **67**, 046609 (2003).
- [7] I. Frank, I. Tamm, Dokl. Acad. Nauk SSSR **14**, 107 (1937).
- [8] J. D. Joannopoulos, R. D. Meade, and J. N. Winn, *Photonic Crystals: Molding the Flow of Light* (Princeton University Press, Princeton, NJ, 1995).
- [9] K. Sakoda, *Optical Properties of Photonic Crystals* (Springer, Berlin, 2001).
- [10] V. P. Bykov, Sov. Phys. JETP **35**, 269 (1972).
- [11] E. Yablonovitch, Phys. Rev. Lett. **58**, 2059 (1987).
- [12] S. John and J. Wang, Phys. Rev. Lett. **64**, 2418 (1990).
- [13] P. St. J. Russell, Appl. Phys. B: Photophys. Laser Chem. **39**, 231 (1986).
- [14] R. Zengerle, J. Mod. Opt. **34**, 1589 (1987).
- [15] H. Kosaka, T. Kawashima, A. Tomita, M. Notomi, T. Tamamura, T. Sato, and S. Kawakami, Phys. Rev. B **58**, R10096 (1998).
- [16] H. Kosaka, T. Kawashima, A. Tomita, M. Notomi, T. Tamamura, T. Sato, and S. Kawakami, Appl. Phys. Lett. **74**, 1212 (1999).
- [17] P. Etchegoin and R. T. Phillips, Phys. Rev. B **53**, 12674 (1996).
- [18] D. N. Chigrin and C. M. Sotomayor Torres, Opt. Spectrosc. **91**, 484 (2001).
- [19] D. N. Chigrin, Phys. Rev. E **70**, 056611 (2004).
- [20] V. A. Belyakov, Nuc. Inst. Meth. Phys. Res. A **248**, 20 (1986).
- [21] F. J. Garcia de Abajo and L. A. Blanco, Phys. Rev. B **67**, 125108 (2003).
- [22] T. Ochiai and K. Ohtaka, Phys. Rev. B **69**, 125106 (2004).
- [23] T. Ochiai and K. Ohtaka, Phys. Rev. B **69**, 125107 (2004).
- [24] K. Yamamoto, R. Sakakibara, S. Yano, Y. Segawa, Y. Shibata, K. Ishi, T. Ohsaka, T. Hara, Y. Kondo, H. Miyazaki, F. Hinode, T. Matsuyama, S. Yamaguchi, and K. Ohtaka, Phys. Rev. E **69**, 045601(R) (2004).
- [25] T. Ochiai and K. Ohtaka, Opt. Express **14**, 7378 (2006).
- [26] F. J. Garcia de Abajo, N. Zabala, A. Rivacoba, A.G. Pattantyus-Abraham, M. O.Wolf, and P.M. Echenique, Phys. Rev. Lett. **91**, 143902 (2003).
- [27] F. J. Garcia de Abajo, A. Rivacoba, N. Zabala, and P. M. Echenique, Phys. Rev. B **68**, 205105 (2003).
- [28] C. Luo, M. Ibanescu, S. G. Johnson, and J. D. Joannopoulos, Science **299**, 368 (2003).
- [29] V. G. Baryshevsky, I. D. Feranchuk, A. P. Ulyanenko, *Parametric X-ray radiation from the electrons in crystals: Theory, Experiment and Applications* (Springer, Heidelberg, 2005).
- [30] J. P. Dowling and C. M. Bowden, Phys. Rev. A **46**, 612 (1992).
- [31] J. D. Jackson, *Classical Electrodynamics* (Wiley, New York, 1975).
- [32] S. G. Romanov, D. N. Chigrin, V. G. Solov'yev, T. Maka, N. Gaponik, A. Eychmuller, A. L. Rogach, C. M. Sotomayor Torres, Phys. Stat. Sol. (a) **197**, 662 (2003).
- [33] S. G. Johnson, and J. D. Joannopoulos, Opt. Express **8**, 173-190, (2001).
- [34] A. Taflov, *Computational Electrodynamics: The Finite-Difference Time-Domain Method* (Artech House, Norwood, 1995).
- [35] J. P. Berenger, J. Comput. Phys. **114**, 185 (1994).
- [36] From the fundamental point of view the parametric X-ray radiation from the moving electron in crystals has very similar physical nature and radiation mechanism, e.g. Ref. [29].
- [37] We use the following definition of direct and inverse Fourier transform:  $f(t) = \frac{1}{2\pi} \int_{-\infty}^{\infty} d\omega f(\omega) e^{-i\omega t}$  and  $f(\omega) = \int_{-\infty}^{\infty} dt f(t) e^{i\omega t}$